Proceedings of the ASME 2017 Power Conference Joint With ICOPE-17
POWER2017-ICOPE-17
June 26-30, 2017, Charlotte, North Carolina, USA

POWER-ICOPE2017-3107

THE EFFECTS OF THE AIR-FUEL VELOCITY RATIO ON TURBULENT NON-PREMIXED BLUFF-BODY FLAMES

Tao Yang
LNM, Institute of Mechanics, Chinese Academy of Sciences
Beijing, 100190, China

Jian Zhang*
LNM, Institute of Mechanics, Chinese Academy of Sciences
Beijing, 100190, China
*Corresponding author: zhangjian@lnm.imech.ac.cn

ABSTRACT

We reported the large-eddy simulations of a series of bluff-body flames varying air-fuel velocity ratio. The air-fuel ratio γ is defined by the ratio of external air velocity to central jet velocity, ranging from 0.05 to 0.50. The case of γ =0.32 is exactly same the Sydney bluff-body HM1e flame. Firstly, the mathematical model and numerical method were validated in details as the simulation results are all in good agreement with measurements in HM1e flame. Then the interaction between turbulence and thermo-chemistry is revealed. As γ increases, external coflow trends to dominant the flame behavior. The stoichiometric mixture fraction shifts from the area between recirculation zone and central jet to the area between external flow and recirculation zone. Corresponding, the flame changes from jet-like, columnar to hat-like flames. The different level of local extinction and reignition is also observed. Local extinction and reignition occurs in jet-like and columnar flames. As γ increases, local extinction becomes easier and reignition becomes harder.

INTRODUCTION

Bluff-body burner is the prototype of many industrial combustors, since it can promote the reactants mix efficiently and extend stable limit. To better understand the intrinsic physics and guide the practical operation of this type of combustor, bluff-body burner has been widely studied, and Sydney bluff-body flame becomes a standard target flame in consideration of well-defined geometry of the burner and its similarity to practical combustors.

The flame structures multi-modally vary with the interaction of the fuel jet and air coflow behind the bluff-body, which are strongly related to the mixing process in the recirculation area [Chen et al (1998), Esquiva et al (2001)]. Vortex shedding and large-scale recirculation are known to keep flame stable in backward facing step and bluff-body wakes [Kim and Pitsch (2006)]. According to experimental studies for bluff-body stabilized flames, the transition from jet-like flame to recirculation flame obviously depends on the inlet flows of air and fuel. This development is linked to a regular evolution from a pure diffusion flame classically stabilized on the burner surface to a partially premixed flame stabilized by recirculating gases in the bluff-body wake. Similar behavior was also found for jet-penetration conditions with a fixed central jet or co-flowing velocity. In the past several decades, the influence of the co-flow on the stabilization process and characterize modes of non-premixed flames has been experimentally studied. All previous works indicate the complicated and close relation among flow structures, mixing characteristics, and flame features. For turbulent bluff-body flames, further investigations of flow structures, scalar mixing, and flame modes under different air/fuel velocity ratio are necessary.

Large-eddy simulation methodology are becoming widely accepted as a high efficient numerical tool for dealing with turbulent reactive flows via resolving energy containing large scale motions and modeling the effects of unresolved small scales and reactions. Among various combustion models, the flamelet progress variable model (FPV) is applied successfully for Sandia flames D-F [Ihme et al (2005)], swirl flames [Ihme et al (2009)] and moderate or intense low oxygen dilution (MILD) combustion [Ihme et al (2012)].

Copyright © 2017 ASME

Downloaded From: http://proceedings.asmedigitalcollection.asme.org/ on 11/02/2017 Terms of Use: http://www.asme.org/about-asme/terms-of-use

The formation of NO and CO in a jet flame and a realistic aircraft engine combustor has been well predicted using FPV [Ihme (2007)].

The focus of current work is on the effects of the air-fuel velocity ratio for turbulent CH_4/H_2 flames stabilized on Sydney bluff-body burner. The predictive capacity of LES/FPV approach is validated via HM1E flame. Results of five bluff-body flames at different air-fuel velocity ratio are compared and analysed to demonstrate the features of various flame modes.

1 MATHEMATICAL MODEL

In LES of turbulent reactive flows combined with FPV approach, the Favre-filtered form of the governing equations (1) can be expressed as [Ihme (2007)]:

$$\tilde{\mathcal{D}}_t \bar{\rho} = -\bar{\rho}\nabla\cdot\tilde{\boldsymbol{u}} \tag{1a}$$

$$\bar{\rho}\tilde{\mathcal{D}}_t\tilde{\boldsymbol{u}} = -\nabla\bar{p} + \nabla\cdot\bar{\underline{\underline{\sigma}}} + \nabla\cdot\bar{\underline{\underline{\sigma}}}^{res} + \bar{\rho}\mathbf{g} \tag{1b}$$

$$\bar{\rho}\tilde{\mathcal{D}}_t\tilde{Z} = -\nabla\left(\bar{\rho}\tilde{\alpha}\nabla\tilde{Z}\right) + \nabla\cdot\bar{\boldsymbol{\tau}}_Z^{res} \tag{1c}$$

$$\bar{\rho}\tilde{\mathcal{D}}_t\tilde{C} = -\nabla\left(\bar{\rho}\tilde{\alpha}\nabla\tilde{C}\right) + \nabla\cdot\bar{\boldsymbol{\tau}}_C^{res} + \bar{\rho}\tilde{\dot{\omega}}_C \tag{1d}$$

$$\bar{\underline{\underline{\sigma}}} = 2\bar{\rho}\tilde{\nu}\left(\tilde{\underline{\underline{S}}} - \frac{1}{3}(\nabla\cdot\tilde{\boldsymbol{u}})\underline{\underline{I}}\right) \tag{2}$$

$$\bar{\underline{\underline{\sigma}}}^{res} = \bar{\rho}\tilde{\boldsymbol{u}}\tilde{\boldsymbol{u}} - \bar{\rho}\widetilde{\boldsymbol{u}\boldsymbol{u}} \tag{3}$$

$$\bar{\boldsymbol{\tau}}_\psi^{res} = \bar{\rho}\tilde{\boldsymbol{u}}\tilde{\psi} - \bar{\rho}\widetilde{\boldsymbol{u}\psi} \tag{4}$$

In the Eqs. (1), the superscript ~ and — represent Favre- and Reynolds-filter quantity, respectively. The subscripts = represents tenor; substantial derivative $\mathcal{D}_t=\partial_t+\ \boldsymbol{u}\bullet\nabla$; $\boldsymbol{u}$, $\boldsymbol{g}$, p, ρ, α represent velocity vector, gravity vector, pressure, density and molecular diffusivity, respectively. Mixture fraction Z and progress variable C are both scalars, ψ is generic scalar variable; In the Eqs. (2), σ is viscous stress, ν is kinematic viscosity, S and I represent rate-of-strain tensor and identity matrix, respectively. Eqs. (3) and (4) are the residual stress tensor and residual scalar flux, respectively, where the superscripts *res* represents subgrid residual quantity. The unclosed terms in the Favre-filtered equations are solved by a dynamic approach [Germano et al (1991)].

In addition to the residual quantities, the filtered density and all other thermochemical quantities are obtained from the FPV approach, which is based on the steady laminar flamelet assumption. The combustion model makes all thermochemical quantities parameterized by a reduced set of scalars to keep the computational cost modest. In steady flamelet equations, the mass fraction Y_i of species i and temperature T can be solved in the mixture fraction space Z [Peters (1984)]:

$$\rho\frac{\chi}{2}\frac{\partial^2 Y_i}{\partial Z^2} + \dot{\omega}_i = 0 \tag{6}$$

$$\rho\frac{\chi}{2}\frac{\partial^2 T}{\partial Z^2} + \sum_{i=1}^{N}\frac{h_i}{c_p}\dot{\omega}_i = 0 \tag{7}$$

$\dot{\omega}_i$ and h_i are the chemical source term and enthalpy for species i, respectively. c_p is mixture specific heat, and N is the number of chemical species. Combining detailed chemical mechanism GRI-Mech2.11 [Bowman et al (1997)], a laminar steady state flamelet library consisted of all thermochemical quantities, $\phi=\varrho_\phi(Z,\ \chi_{st}\ )$, where χ_{st} is the stoichiometric scalar dissipation rate, can be set up to supply some thermal quantities in the equations(1). The steady flamelet model is extended to the flamelet progress variable (FPV) approach by Pierce (2004) through introducing a reactive progress parameter to transfer ϕ from $\varrho_\phi(Z,\chi_{st})$ to $\varrho_\phi(\ Z,\ C)$ for considering extinction and re-ignition effects [Ihme et al (2005)]. In the present work, the progress variable C was defined as a linear combination of four major product mass fractions:

$$C = Y_{CO} + Y_{CO_2} + Y_{H_2} + Y_{H_2O} \tag{8}$$

The sub-grid scale interaction of turbulence and chemistry can be modeled by an assumed joint probability density function (PDF) approach, where the mixture fraction Z subjects to β distribution and the progress variable C follows δ distribution. The Favre-filtered thermochemical quantities, such as reactive source, temperature and species etc. can be obtained through integrating the laminar steady state flamelet library [Ihme (2007)]:

$$\begin{aligned}\tilde{\phi} &= \iint \varrho_\phi(Z,C)\,\tilde{P}(Z,C)\,dZdC \\ &= \tilde{\varrho}_\phi\left(\tilde{Z}, \widetilde{Z''^2}, \tilde{C}\right)\end{aligned} \tag{9}$$

2 EXPERIMENTAL AND NUMERICAL SETUP

2.1 Experimental setup

Sydney bluff-body burner consists of a cylindrical bluff-body with an orifice and is centered in a wind tunnel that supports a co-flowing air stream. The bluff-body diameter is $D=D_b$=50mm and the fuel jet diameter is D_j=3.6mm. The central nozzle ejects a turbulent fuel jet at Re=15800 which is composed of methane and hydrogen (1:1 by volume) with a stoichiometric mixture fraction Z_{st}=0.05. U_e and U_j represent the fuel jet velocity and the external ambient coflow velocity, respectively.

2.2 Numerical setup

As shown in Fig.1, the domain extends from 0 to $80D_j$ in the axial direction, from 0 to $24D_j$ in the radial direction, and from 0 to 2π radians in the azimuthal direction. Bluff-body flames are investigated by using a cylindrical coordinate system

Copyright © 2017 ASME

Downloaded From: http://proceedings.asmedigitalcollection.asme.org/ on 11/02/2017 Terms of Use: http://www.asme.org/about-asme/terms-of-use

based on conservative, second-order finite-volumes on staggered grids. A second-order, semi-implicit time advancement approach is used. The outlet boundary uses convective boundary condition. The wall boundary adopts no-slip Dirichlet conditions for velocity, and Neumann conditions for all scalars and pressure.

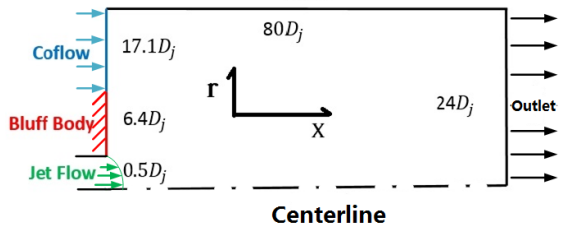

Figure1 The computational domain

For the central inflow profiles of simulations, a separate LES of a periodic pipe flow supports the fully developed turbulent fuel jet by enforcing the same bulk axial velocity with the experiment. A plug flow is set as the inlet profile for the annular air coflow.

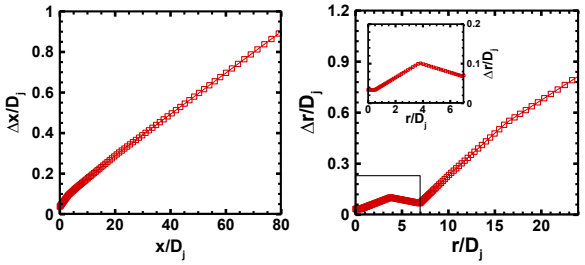

Figure 2 Grid stretching diagrams for axial(left) and radial (right) directions

In order to resolve enough turbulent kinetic energy and capture key flow characteristics for bluff body flames, the computational domain is divided by 256×165×64 control volumes in axial, radial and circumferential directions. As shown in Fig.2, the axial grid is refined in the recirculating zone and is stretched from *x/D*=1.2 to the end. The unevenly spaced grid points in radial direction are concentrated in the shear layer region surrounding the fuel jet and edge of bluff body. The circumferential grid is discretized uniformly. The current grid-resolution could be called a *fine* grid and resolve a sufficient amount of the turbulent kinetic energy according to Refs.[Kempf et al (2006)]. The numerical simulation is run over dozens of flow-through-times up to obtain a statistically stationary flow field, and statistics are collected over 10 flow-through-times. The present study employs 16 CPUs for 2.7 million cells on the computing platform of National Super Computing Center in Tianjin (NSCC-TJ).

2.3 Simulation cases

The present study is investigated over a wide range values of mean external air velocity, $U_e = U_{Air}$ under the condition that mean fuel jet velocity, $U_j = U_{Fuel}$ is fixed. The inlet velocities of five simulation cases are shown in Table 1. The velocity ratio of air and fuel, γ ranges from 0.05 to 0.50, where the fourth case is Sydney bluff-body flame HM1E, of which measurement data is available from Masri (2011).

Table 1 Simulation Cases

	(1)	*(2)*	*(3)*	*(4)*	*(5)*
U_{Air}（m/s）	5.4	10.8	21.6	34.6	54
U_{Fuel}（m/s）	108	108	108	108	108
$\gamma = U_{Air}/U_{Fuel}$	0.05	0.1	0.2	0.32	0.5

3 RESULTS AND DISCUSSIONS

In this section, all statistical data are collected after reaching the statistically stationary state. Firstly, the predictive results for Sydney bluff-body flame HM1e are validated with measurements. Secondly, structures of bluff-body flame are presented via comparing their temperature and mixture fraction fields with the increase of air-fuel velocity ratio.

3.1 Validation of bluff-body flame HM1E

Radial profiles of mean temperature and species mass fractions at three axial locations are shown in Fig.3. The numerical simulation is in overall good agreement with measurements up to the end of neck zone, corresponding to *x/D*=1.8. The slight under-predictions for temperature and OH at all considered locations are mainly due to using an adiabatic combustion model and not considering wall heat loss effects [Kempf et al (2006), Ihme and Pitsch (2009)]. The computed CO at the centerline is slightly overpredicted downstream of the recirculation zone. The discrepancies may result from flamelet regime or a cumulative effect of the sub-filter modeling errors [Raman and Pitsch (2005)]. The trend and order of NO are in accordance with experimental data, while the errors are obvious and may derive from and noninclusion of radiation heat loss for the steady state flamelet formulation [Ravikanti et al (2008)]. Overall, the structure and combustion products of the bluff-body flame could be captured accurately by the current mathematical model. The remaining section will present effects of the air/fuel velocity ratio on turbulent non-premixed bluff-body flames.

3.2 Flame structures in bluff-body burner

Based on well prediction of HM1e flame, we will present here four more cases in addition to HM1e flame, changing velocity ratio γ from 0.05 to 0.5.

Copyright © 2017 ASME

Downloaded From: http://proceedings.asmedigitalcollection.asme.org/ on 11/02/2017 Terms of Use: http://www.asme.org/about-asme/terms-of-use

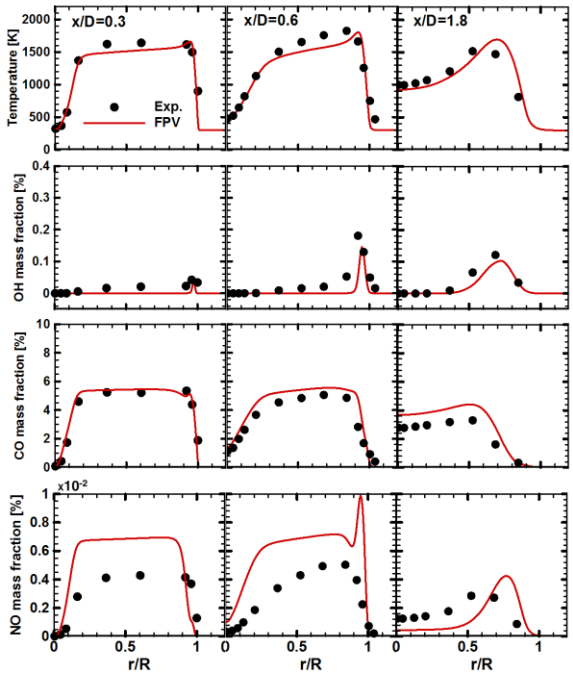

Figure 3 Comparison of measured(●) and calculated (—) mean statistics of temperature T, hydroxyl radical OH, carbon monoxide CO and nitric monoxide NO at different axial locations in the Sydney HM1E flame.

The selective range of γ accords to a regime of the bluff-body flame from a jet-like flame to a recirculation flame. Through these five flames, we aim to provide a comprehensive observation about the interaction between turbulence and thermo-chemistry in bluff-body burner.

1) Jet-like flame and recirculation flame

In bluff-body burner, jet-like flame and recirculation flame are two typical flames. The former is the case of that external flow rate is so low that central jet has not been affected and the flame seems like a jet flame. The latter is just on the contrary, where the external flow rate is so high that central jet is confined by external flow and the flame shows a recirculation flame.

The flame structures are shown in Fig. 4a. The left flame is for the case of γ =0.05 and the right is for γ =0.5. In this paper, the cases of γ =0.05 and 0.50 correspond jet-like flame and recirculation flame, respectively. For each flame, left side is time-averaged temperature field and right side is a snapshot of temperature field. Dashed line corresponds to stoichiometric mixture fraction Z_{st}=0.05. For jet-like flame, the flame showed a lifted jet flame. Nonetheless, there still is a little difference from free-jet flame that a small neck zone at x/D=0.8 is found. Neck zone is found that it associated with local extinction in bluff-body flames [Kim and Pitsch (2006)]. Here we will show the local extinction and reignition by hydroxyl distribution in Fig. 4b.

The contour of OH mass fraction with dashed Z_{st} line is plotted for the jet-like flame and recirculation flame. In the case of γ =0.05, along the Z_{st} line a low OH zone emerges after a high OH zone and the other high OH zone is following. This pattern accords to the process of that the production of OH is suppressed since local extinction and re-produces until flame reignites. When γ =0.5, on the contrary, local extinction vanishes.

2) The structure of the five flames

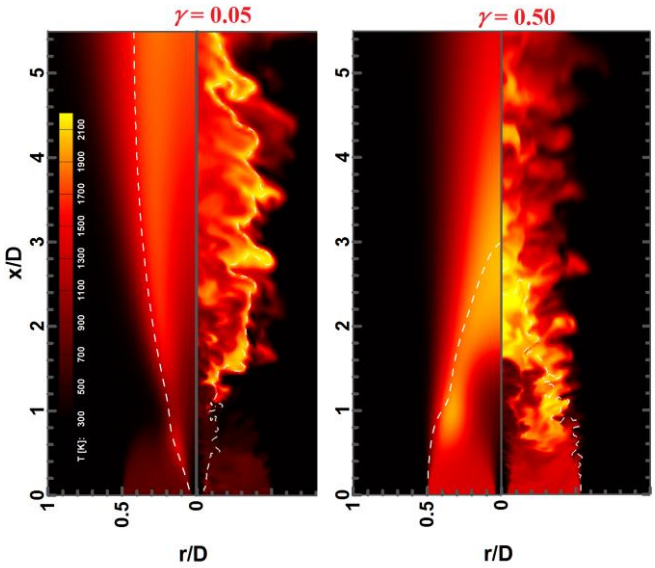

(a) Time-averaged (left half) and instantaneous (right half) temperature

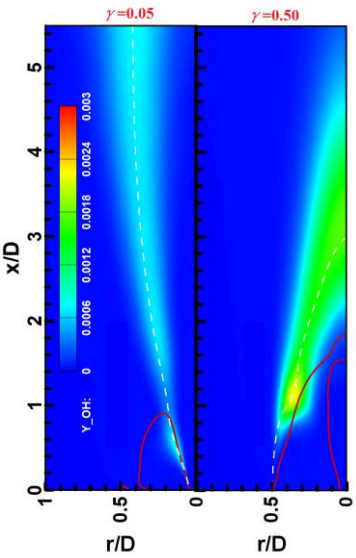

(b) Time-averaged OH mass fraction

Copyright © 2017 ASME

Downloaded From: http://proceedings.asmedigitalcollection.asme.org/ on 11/02/2017 Terms of Use: http://www.asme.org/about-asme/terms-of-use

Figure 4 The temperature(a) and hydroxyl(b) contours of γ=0.05 and 0.50 bluff-body flames; Dash-dot line correspond to stoichiometric mixture fraction Z_{st}=0.05; Red line represents zero axial velocity.

The flame transition from jet-like flame into recirculation flame with increasing of velocity ratio is essentially the result of the interaction between turbulence and thermo-chemistry in bluff-body burner. Plotting the five flame structures and mixture fraction field in Fig.5a and Fig.5b respectively, we will explore the transition process in details.

As we described before, at a lower coflow velocity, the bluff-body flame seems like a lifted jet flame. There is no obvious heat release in the recirculation zone. The increasing of coflow velocity improves the mixing of reactants, and enhances chemical reactions near to the bluff-body. Along with that local extinction can be observed apparently at the neck zone of flame and re-ignition happens intermittently further downstream. Due to the shift of the stoichiometric isoline, the flame moves toward the downstream and outside. The pattern of bluff-body flames, which are composed of upstream recirculation-dominated part and downstream jet-like part, becomes columnar. A further increasing in air coflow velocity induces a recirculation flame, in which the fuel jet is completely confined by the recirculation zone. The length of recirculation flame in hat-like shape becomes very short. The transition of flame patterns in this work is similar to the description of Fig.10 from the Ref. [Esquiva et al (2001)], in which the fixed central gas jet is laminar (Re=1800) and bluff-body-stabilized non-premixed flames exhibit five characteristic modes: laminar flame, transition I, laminar ring flame, transition II, and recirculating flame. The former two modes are classified into the fuel-jet-dominant state. The last recirculating flame is dominated by the air-flow. Other modes are a fine match between fuel-jet and air-flow dominant conditions. According to the variance of flame structures at different velocity ratio of annular to central jets, a combustion diagram for bluff-body flames was classified into five flame modes: recirculation zone flame, central-jet dominated flame, jet-like flame, partially quenched flame, lifted flame[Chen et al (1998)]. Combined with mentions above, similar patterns can be found for either turbulent or laminar central-jet bluff-body flames, even though the bluff-body geometry and fuel are not same completely.

For non-premixed flames, the mixing of the reactants primarily determines the location of the flame front. The evolution of flame modes with γ is related to a displacement of stoichiometric mixture fraction [Esquiva et al (2001)]. Under differentγ conditions, the distributions of the mixture fraction exhibit complex changes as shown in Fig. 5b. With the increasing of the air-fuel velocity ratio, stoichiometric mixtures move outward from the fuel side to the outer edge of the recirculation zone, and wraps gradually the recirculating line, defined U=0 which characterized recirculation region inside. The mixture in recirculation zone distributes generally uniform, so in the most cases the Z_{st} line does not across recirculation zone. In the only case of γ =0.10, Z_{st} isoline does, which results in high temperature inside recirculation zone.

As shown Fig.5c, these five flames also show different level of local extinction and reignition through OH distribution. Local extinction and reignition is mainly occurs whenγ is lower than 0.32. As γ increases from γ =0.05 to γ =0.20, the local extinction getting more intense and reignition branch is getting weaker. This phenomenon could be explained by the physics that as coflow velocity increases, the scalar dissipation in neck zone becomes higher, flame hardly sustains, so does reignition at downstream. At γ =0.32, coflow velocity is so large that wraps central jet, and neck zone disappears, flame thus shows no obvious local extinction and reignition.

4 CONCLUSIONS

Large eddy simulations of five flames in Sydney bluff-body burner were performed. The Sydney bluff-body flame HM1E is compared with the experimental data to validate the flamelet progress variable approach. Three characteristic modes of turbulent bluff-body flames are observed and reported with different air/fuel velocity ratio, γ . The conclusions can be drawn below:

1) The interaction between turbulence and thermo-chemistry is explored by varying velocity ratio of external flow to central jet.

2) As γ increases, the stoichiometric mixture fraction shifts from the area between recirculation zone and central jet to the area between external flow and recirculation zone. With the shift, bluff-body flames change from jet-like, columnar to hat-like flames.

3) Bluff-body flames exhibit different level of local extinction and reignition. Local extinction and reignition occurs in jet-like and columnar flame. As γ increases, local extinction becomes easier and reignition becomes harder.

Copyright © 2017 ASME

Downloaded From: http://proceedings.asmedigitalcollection.asme.org/ on 11/02/2017 Terms of Use: http://www.asme.org/about-asme/terms-of-use

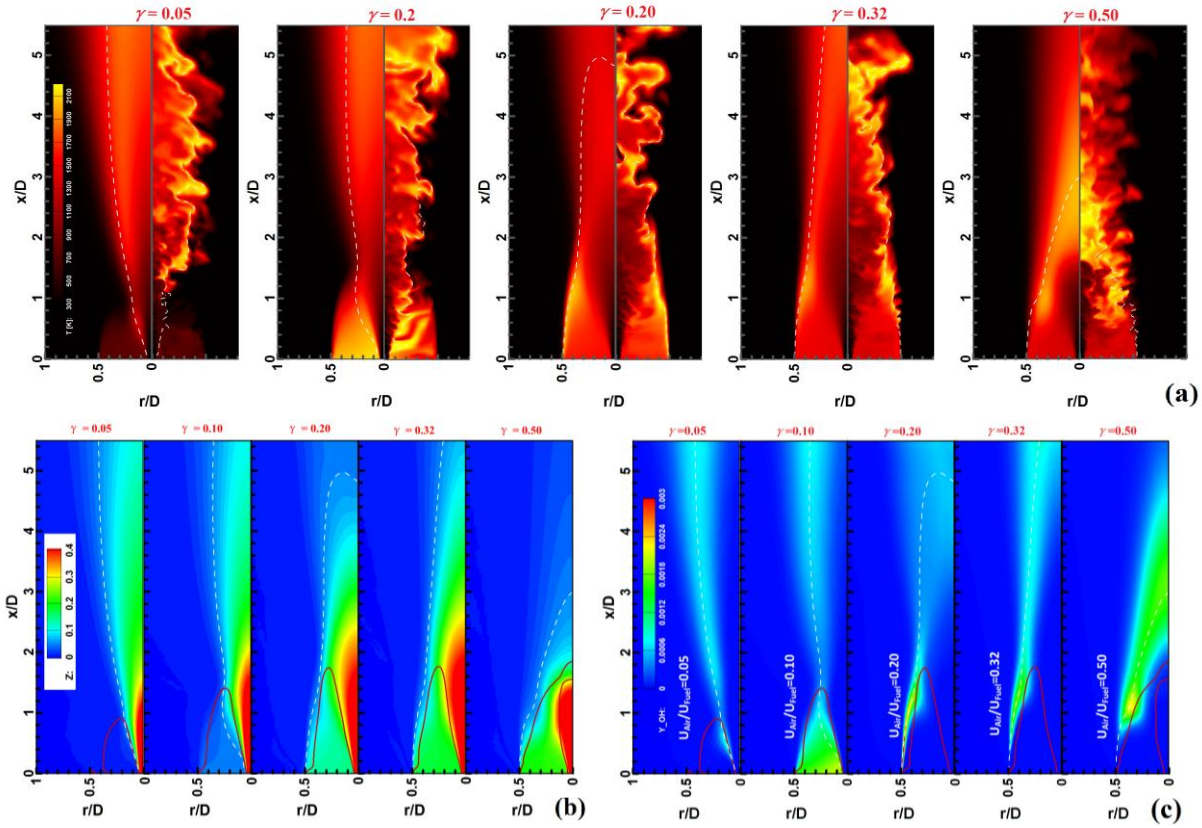

Figure 5 Time-averaged (left half) and instantaneous (right half) temperature(a), time-averaged mixture fraction(b) and time-averaged hydroxyl (c) fields for the five flames fromγ=0.05 to γ=0.50; Dash-dot: the stoichiometric mixture fraction Zst=0.05; Red line: zero axial velocity U=0.

ACKNOWLEDGEMENTS

The investigations presented in this paper have been supported by National Natural Science Foundation of China under contract 51376190，11572330，and 51306013. The authors also acknowledge National Supercomputer Centre in Tianjin for providing computational resource.

REFERENCES

Bowman C. T., Hanson R. K., Davidson D. F., Gardiner W. C., Lissianski V., Smith G. P., Golden, D. M., Frenklach M. and Goldenberg M. (1997). GRI-Mech2.11. http://www.me.berkeley.edu/gri- mech/.

Chen Y. C., Chang C. C., Pan K. L. and Yang J. T. (1998). Flame lift-off and stabilization mechanisms of non-premixed jet flames on a bluff-body burner, *Combustion and Flame*, 115(1), pp. 51-65.

Dally B. B., Masri A. R., Barlow R. S. and Fiechtner G. J. (1998). Instantaneous and mean compositional structure of bluff-body stabilized non-premixed flames, *Combustion and Flame*, 114(1–2), pp. 119-148.

Esquiva D. I., Nguyen H. T. and Escudie D. (2001). Influence of a bluff-body's shape on the stabilization regime of non-premixed flames, *Combustion and Flame*, 127(4), pp. 2167-2180.

Germano M., Piomelli U., Moin P., and Cabot W. H. (1991). A dynamic subgrid-scale eddy viscosity model. *Physics of Fluids A*, 3(7), pp. 1760-1765.

Ihme M., Cha C. M. and Pitsch H. (2005). Prediction of local extinction and re-ignition effects in non-premixed turbulent combustion using a flamelet/ progress variable approach. *Proceedings of the Combustion Institute*, 30(1), pp. 793-800.

Ihme M. (2007). Pollutant formation and noise emission in turbulent non-premixed flames. PhD thesis, Stanford University.

Ihme M., Schmitt C., and Pitsch H. (2009). Optimal artificial neural networks and tabulation methods for chemistry representation in LES of a bluff-body swirl-stabilized flame. *Proceedings of the Combustion Institute*, *32*(1), pp. 1527-1535.

Ihme M., Zhang J., He G., and Dally B. (2012). Large-eddy simulation of a jet-in-hot-coflow burner operating in the oxygen-diluted combustion regime. *Flow, turbulence and combustion*, *89*(3), pp. 449-464.

Copyright © 2017 ASME

Downloaded From: http://proceedings.asmedigitalcollection.asme.org/ on 11/02/2017 Terms of Use: http://www.asme.org/about-asme/terms-of-use

Kempf A., Lindstedt R. P. and Janicka, J. (2006). Large-eddy simulation of a bluff-body stabilized non-premixed flame, *Combustion and Flame*, 144 (1), pp. 170-189.

Kim S. H., and Pitsch H. (2006). Mixing characteristics and structure of a turbulent jet diffusion flame stabilized on a bluff-body. *Physics of Fluids*, *18*(7), pp. 075-103.

Masri A. R. (2011). Web site for the Sydney bluff-body flame series. http://www.aeromech.usyd.edu.au/thermofluids.

Peters N. (1984). Laminar diffusion flamelet models in non-premixed turbulent combustion. *Progress in Energy and Combustion Science*, 10(3), pp. 319-339.

Pierce C. D. and Moin P. (2004). Progress-variable approach for large-eddy simulation of nonpremixed turbulent combustion. *Journal of Fluid Mechanics*, 504, pp. 73-97.

Raman V. and Pitsch H. (2005). Large-eddy simulation of a bluff-body stabilized non-premixed flame using a recursive filter-refinement procedure. *Combustion and Flame*, 142(4), pp. 329-347.

Ravikanti M., Malalasekera W., Hossain M., and Mahmud T. (2008). Flamelet based NO_x radiation integrated modelling of turbulent non-premixed flame using Reynolds-stress closure, *Flow, Turbulence and Combustion*, 81(1-2),pp. 301-319.

Yang J. T., Chang C. C., and Pan, K. L. (2002). Flow structures and mixing mechanisms behind a disc stabilizer with a central fuel jet. *Combustion Science and Technology*, 174(3), pp. 93-124.

Yang J. T., Chang C. C., Pan K. L., Kang Y. P., and Lee Y. P. (2002). Thermal analysis and PLIF imaging of reacting flow behind a disc stabilizer with a central fuel jet. *Combustion Science and Technology*, *174*(3), pp. 71-92

Copyright © 2017 ASME

Downloaded From: http://proceedings.asmedigitalcollection.asme.org/ on 11/02/2017 Terms of Use: http://www.asme.org/about-asme/terms-of-use